Analysis of Azimuthal Doppler Shift of Anisotropically Absorbed Laguerre-Gaussian Beam Propagating in Transverse Flow

Hiroki MINAGAWA, Shinji YOSHIMURA[1,2], Kenichiro TERASAKA[3] and Mitsutoshi ARAMAKI

College of Industrial Technology, Nihon University, Narashino, Chiba 275-8575, Japan
[1] *National Institute for Fusion Science, National Institutes of Natural Sciences, Toki, Gifu 509-5292, Japan*
[2] *Center for Low-temperature Plasma Sciences, Nagoya University, Nagoya 464-8601, Japan*
[3] *Interdisciplinary Graduate School of Engineering Sciences, Kyushu University, Kasuga, Fukuoka 816-8580, Japan*

(Received 27 July 2022 / Accepted 13 August 2022)

The particle flux onto a material is an important parameter in the study of the plasma-material interaction. With conventional Doppler spectroscopy, it is difficult to measure the flow velocity perpendicular to the material because only the velocity component projected on the wave number vector can be measured. To overcome the limitation, we are developing a transverse flow measurement method using the azimuthal Doppler shift of a Laguerre-Gaussian (LG) beam absorption spectroscopy. In this paper, the feasibility of this spectroscopy method has been examined by numerical analysis. The LG beam is anisotropically absorbed in the transverse flow due to the azimuthal Doppler shift. Since the anisotropic LG beam rotates with propagation, the spatial structure of resonance absorption in plasma and the intensity structure of the LG beam that has propagated through the plasma are inevitably different in the LG beam absorption spectroscopy. It was shown that the deviation from the original azimuthal Doppler shift is reduced to several percent at the position where the intensity distribution of the LG beam reaches its maximum value. Therefore, the transverse flow can be measured with sufficient accuracy by properly selecting the position on the beam cross-section used to evaluate the azimuthal Doppler shift.

© *2022 The Japan Society of Plasma Science and Nuclear Fusion Research*

Keywords: Laguerre-Gaussian beam, optical vortex, azimuthal Doppler shift, angular spectrum method, tunable diode laser absorption spectroscopy

DOI: 10.1585/pfr.17.1401099

1. Introduction

High-resolution spectroscopies using the resonant excitation of atoms with the narrow-band tunable diode lasers are valuable methods to measure Doppler spectra for plasma dynamics study [1–4]. In conventional laser spectroscopy, it has been taken for granted that the observed Doppler spectrum is the projection of the velocity distribution function onto the wave vector of the excitation laser. Therefore, the measurements are recognized as impossible when the optical path parallel to the desired velocity direction is not available. The limitation of the observable degree of freedom is unfavorable for studying plasma-surface interactions such as the sheath dynamics, heat flux to the wall of a fusion reactor, or surface reactions in plasma processing, since the probe laser is required to be entered perpendicular to the surface to measure the particle flux to the surface [5, 6]. This limitation comes from the fact that the phase plane of the excitation laser is approximated to be flat; however, it can be overcome by using a probe beam whose wavefront has a three-dimensional structure. The authors have been developing a spectroscopy method to measure the flow perpendicular to the wave vector using a Laguerre-Gaussian (LG) beam [7, 8]. This spectroscopy method can ease the strong connection between the propagation direction of the probe beam and the observable velocity component and help the study of plasma-surface interactions. In this paper, we numerically analyze the LG beam propagation while being anisotropically absorbed by the transversely flowing plasma, and the feasibility of the application in the transverse flow measurement is discussed.

The LG mode electromagnetic waves are cylindrically-symmetric solutions of the Helmholtz wave equation with a paraxial approximation in free space [9]. The electric field of the LG mode propagating in the z-direction is expressed by

$$E_{\ell p}(r,\phi,z) = u_{\ell p}(r,\phi,z)\exp[i(kz-\omega t)].$$

$$u_{\ell p}(r,\phi,z) = \sqrt{\frac{2p!}{\pi(p+|\ell|)!}}\left(\frac{\sqrt{2}r}{w(z)}\right)^{|\ell|} L_p^{|\ell|}\left[\frac{2r^2}{w(z)^2}\right]\frac{w_0}{w(z)} \times\exp\left[-\frac{r^2}{w(z)}\right]\exp[i\ell\phi] \times\exp\left[-i(1+2p+|\ell|)\tan^{-1}\left(\frac{z}{z_R}\right)\right]\exp\left[i\frac{kr^2}{2R(z)}\right], \tag{1}$$

where k is the wavenumber, ω is the angular frequency,

author's e-mail: aramaki.mitsutoshi@nihon-u.ac.jp

© 2022 The Japan Society of Plasma Science and Nuclear Fusion Research

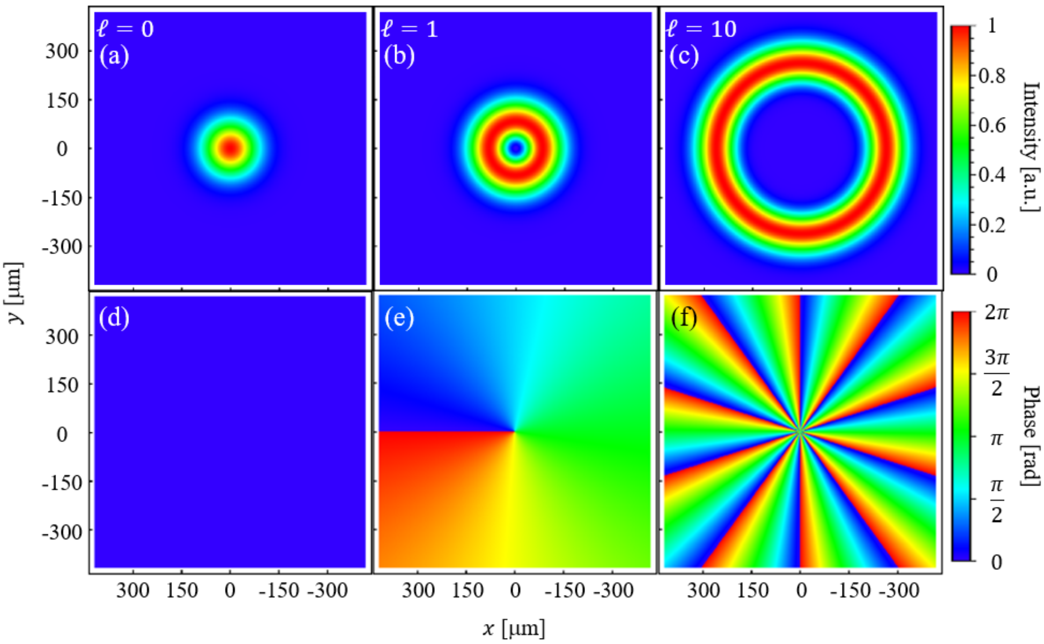

Fig. 1 Intensity distributions and phase distributions of LG beams with $\ell = 0, +1, +10$. In the case of $\ell \neq 0$, the intensities have donut-shaped distribution, and the phase varies by $2\pi\ell$ in the azimuthal direction.

$L_p^\ell[x]$ is the associated Laguerre polynomial, $w(z)$ is the beam radius of the lowest-order mode, $w_0 = w(0)$ is the beam waist, z_R is the Rayleigh range, and $R(z)$ is the curvature of the wavefronts. In this paper, we assume the radial index $p = 0$. Figures 1 (a) - (c) show intensity $I_{\ell 0} = |E_{\ell 0}|^2$ and (d) - (f) show phase distribution $\mathrm{Im}(u_{\ell p})$ at $z = 0$ with the azimuthal index ℓ (topological charge) $= 0, 1$ and 10, respectively. The lowest order mode ($p = 0$, $\ell = 0$) has the Gaussian intensity distribution, and its phase is uniform in the beam cross-section. The beam waist w_0 is assumed to be 117 µm. When $\ell \neq 0$, the phase varies in the azimuthal direction with the term of $\exp(i\ell\phi)$. Since the center of the beam is the phase singularity, the intensity profile has a donut shape. As mentioned in a later section, we use an LG beam with $\ell = 10$ in our experiments, and its radius to the maximum intensity position from the center of the LG beam is 262 µm. In the following sections, we first describe the anisotropic resonant absorption of the LG beam due to the azimuthal Doppler shift in the uniform transverse flow. Next, we numerically analyze the propagation of the anisotropically absorbed LG beam using the angular spectrum method [10–14]. The effect of the rotation of the complex amplitude distribution due to the Gouy phase shift on the structure of the anisotropically absorbed intensity distribution is evaluated. We also discuss the feasibility of the transverse flow velocity measurement using the azimuthal Doppler shift under the parameters of our experimental setup. Finally, conclusions are given in Sec. 5.

2. Anisotropic Resonant Absorption of LG Beam in Transverse Flow

Since the longitudinal Doppler shift occurs due to the movement crossing the wavefront, the conventional tunable diode laser absorption spectroscopy (TDLAS) using a plane wave can only detect the movement in the beam propagating direction. In addition, the Doppler shift and the absorption coefficients are uniform over the beam cross-section. On the other hand, since the LG beam has a spiral wavefront, the resonance absorption conditions of the particles moving in the LG beam are subjected to the Doppler shift that depends on the three velocity components of the cylindrical coordinate system, as shown in the following equation [15].

$$\delta_{LG} = -\left[k + \frac{kr^2}{2(z^2+z_R^2)}\left(\frac{2z^2}{z^2+z_R^2} - 1\right) - \frac{(2p+|\ell|+1)z_R}{z^2+z_R^2}\right] v_z - \left(\frac{krz}{z^2+z_R^2}\right) v_r - \left(\frac{\ell}{r}\right) v_\phi \,, \qquad (2)$$

where v_z, v_r, v_ϕ is the velocity component of the atom in the axial, radial, azimuthal direction, δ_{LG} is the Doppler shift in the angular frequency. Since we use a collimated LG beam for spectroscopy in the vicinity of the beam waist, we approximate Eq. (2) as follows by assuming $r, z < z_{\mathrm{R}}$.

$$\delta_{LG} \approx -kv_z - \left(\frac{\ell}{r}\right) v_\phi. \qquad (3)$$

The first term is the traditional Doppler shift, and the second term is the azimuthal Doppler shift we intend to use for the beam crossing particle flow measurement. Figure 2 shows a two-dimensional distribution of the azimuthal Doppler shift for the resonance absorption of the excitation laser. It is calculated with the wavelength $\lambda = 697$ nm for the absorption measurement of metastable-state argon atoms $((^2P^0_{2/3})4s \rightarrow (^2P^0_{1/2})4p)$, $\ell = 10$ and $U_x = 3000$ m/s. In Fig. 2, the sign of the Doppler shift is opposite to Eq. (3), since the blue shift for the atom corresponds to the red shift for the excitation laser. Since the azimuthal component of U_x is $-U_x \sin\phi$, the azimuthal Doppler shift depends on the ℓ, r, and ϕ. Therefore, the resonance absorption of the LG beam is also anisotropic. To calculate the Doppler spectrum, we assume the velocity distribution function of the flowing atoms as a shifted-Maxwellian in the cylindrical coordinate system.

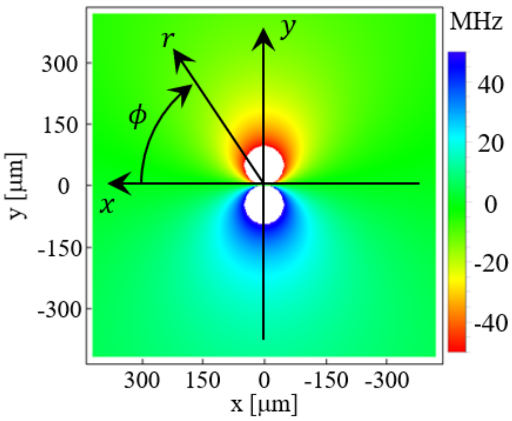

Fig. 2 Doppler shift distribution occurring on the cross-section of the LG beam with $\ell = 10$.

$$f(v_z, v_r, v_\phi) = \left(\frac{m}{2\pi k_B T}\right)^{\frac{3}{2}} \times \exp\left[-\frac{m\left((v_z-U_z)^2 + (v_r-U_r)^2 + (v_\phi-U_\phi)^2\right)}{2k_B T}\right], \tag{4}$$

where k_B is the Boltzmann constant, m is the mass of the atom, T is the gas temperature, U_z, U_r, U_ϕ are the flow velocity in each direction. Assuming the flow only in the x-direction and ignoring the Doppler shift due to the velocity component in the r direction, the shape of resonance absorption distribution seen from the atoms is as follows [8]:

$$f_{\mathrm{atm}}(\delta_{LG}) \propto \left(\frac{r^2}{\ell^2 + k^2 r^2}\right)^{\frac{1}{2}} \times \exp\left[-\frac{m}{2k_B T}\frac{r^2}{\ell^2 + k^2 r^2}\left(\delta_{LG} - \frac{\ell}{r}U_x \sin\phi\right)^2\right]. \tag{5}$$

Since the frequency shift is inverted when viewed from the excitation laser, the Doppler spectrum of the absorption spectroscopy is as follows.

$$f_{\mathrm{abs}}(\delta_{LG}) = \alpha_0 k \left(\frac{r^2}{\ell^2 + k^2 r^2}\right)^{\frac{1}{2}} \times \exp\left[-\frac{m}{2k_B T}\frac{r^2}{\ell^2 + k^2 r^2}\left(\delta_{LG} + \frac{\ell}{r}U_x \sin\phi\right)^2\right], \tag{6}$$

where α_0 is the absorption coefficient at the resonance center when r is infinite. The transverse gas flow velocity is

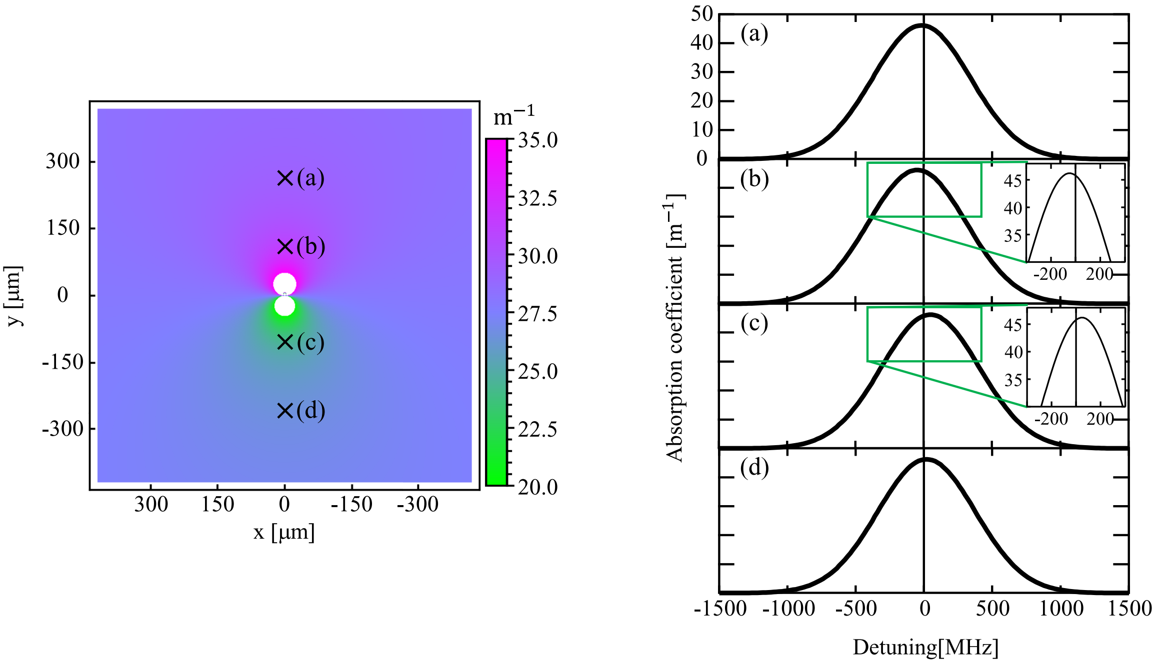

Fig. 3 The absorption coefficient distribution in the beam cross-section. The laser frequency is detuned by +360 MHz from the resonance center. The absorption spectra of the LG beam at the points (a) ($y = 262$ μm), (b) ($y = 100$ μm), (c) ($y = -100$ μm), (d) ($y = -262$ μm) are shown in right panels.

obtained from the azimuthal Doppler shift $-(\ell/r)U_x \sin\phi$ of the spectrum. The left panel of Fig. 3 shows the spatial distribution of f_{abs} at +360 MHz detuning from the resonance center. The gas temperature is 300 K, α_0 is 46 m^{-1}, and the other parameters are the same as the calculation in Fig. 2. The LG beam propagating in the transverse gas flow is deformed into an anisotropic intensity profile by the absorption-coefficient distribution shown in Fig. 3. Figures 3 (a) - (d) are Doppler spectra obtained from the detuning frequency dependence of the absorption coefficient at each location. The azimuthal Doppler shift is visible in Figs. 3 (b) and (c).

3. Propagation of Anisotropically Absorbed LG Beam

Hamazaki et al. showed that the partially cut LG beam rotates due to the Gouy phase shift while propagating in free space [16]. In a similar way, the LG beam propagating while being anisotropically absorbed in the plasma will rotate with a Gouy phase shift. Therefore, the absorption distribution of the LG beam observed after propagating through the plasma will be rotated from the original absorption coefficient distribution in Fig. 3. In this section, we examine the effect of the rotation of the absorption structure on the transverse flow measurement by numerically analyzing the LG beam propagation using the angular spectrum method. The angular spectrum method is formulated as follows [10–14]:

$$g(x,y,z)=\mathcal{F}^{-1}\left[\mathcal{F}[g(x,y,0)]\exp\left[i2\pi(\lambda^{-2}-f_x^2-f_y^2)^{1/2}z\right]\right], \quad (7)$$

where λ is the wavelength, $g(x,y,0)$ and $g(x,y,z)$ are the initial and the propagated complex amplitude field, $\mathcal{F}$ and $\mathcal{F}^{-1}$ is the Fourier transform and the inverse Fourier transform, f_x and f_y are the spatial frequencies on the x-y plane. We performed the numerical calculation assuming that the LG beam enters the plasma at the beam waist (z = 0 mm), α_0 = 34 m^{-1}, the absorption length is 15 mm, and the other parameters are the same as the calculation in Fig. 3. The absorption and propagation are repeatedly evaluated with the propagation step of 2λ (= 2 × 693 nm). Figures 4 (a) and (b) show the intensity distribution and the absorption ratio distribution at z = 15 mm, respectively. Since the laser frequency is positively detuned, the lower part of the beam is absorbed more than the upper part in Fig. 4 (a). The anisotropic intensity distribution rotated clockwise by 0.12 rad. The rotation angle is approximately half of the Gouy phase shift for the 15 mm propagation since the beam is gradually absorbed as it propagates through the plasma. The Doppler spectra at z = 15 mm are constructed by calculating the LG beam propagation at several detuning frequencies. Figure 5 shows the distribution of the azimuthal Doppler shift obtained from the spectra at z = 15 mm. Although the resonance absorption frequency of the LG beam shifted by the azimuthal Doppler shift is symmetrical about

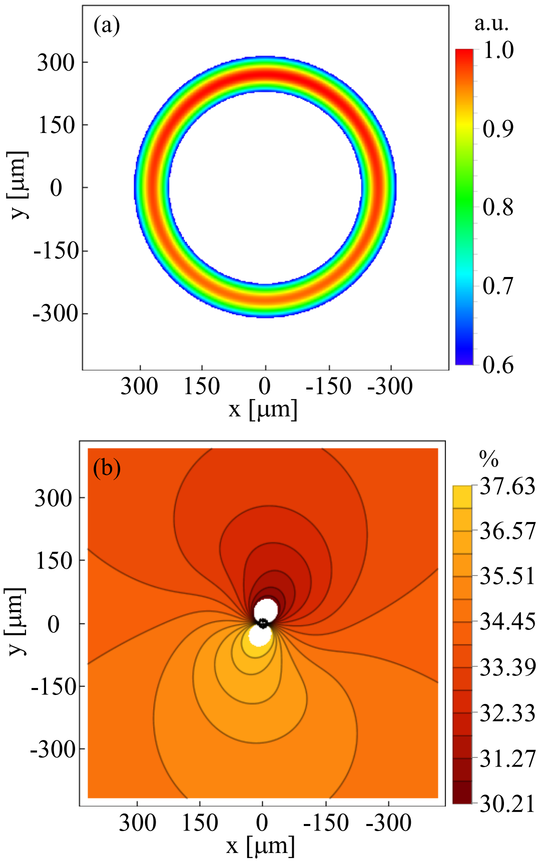

Fig. 4 (a) The Intensity distribution of the anisotropically absorbed LG beam. (b) The absorption ratio distributions.

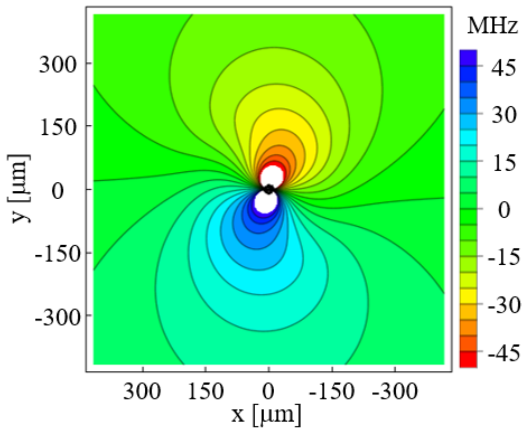

Fig. 5 Doppler shift distribution deformed by the beam structure rotation.

the y-axis, as shown in Fig. 2, the observable azimuthal Doppler shift distribution is inevitably rotated due to the Gouy phase shift, as shown in Fig. 5.

Figure 6 shows the ϕ dependence of the azimuthal Doppler shift at r = 100 μm and 262 μm. The broken lines indicate the original azimuthal Doppler shift, $-(\ell/r)U_x \sin\phi$, shown in Fig. 2, and the solid lines show the azimuthal Doppler shift obtained from the spectra at

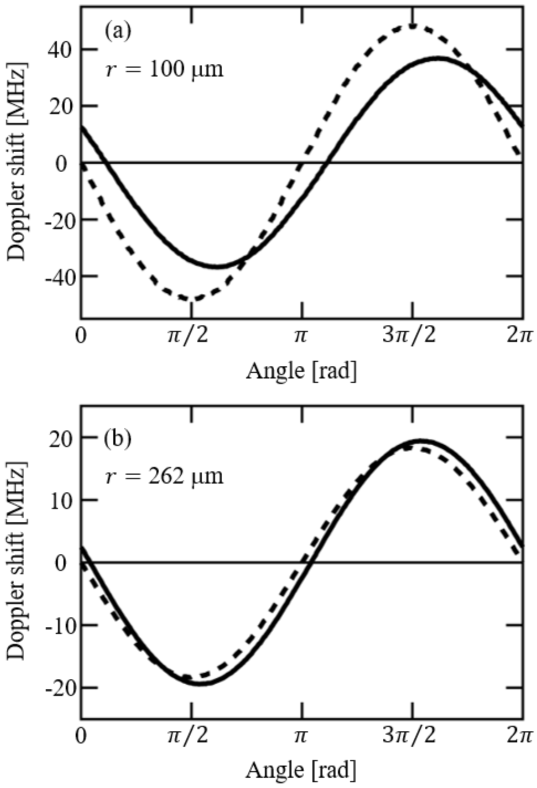

Fig. 6 The ϕ dependence of the azimuthal Doppler shift at (a) $r = 100\,\mu$m and (b) $262\,\mu$m. The broken lines show the original azimuthal Doppler shift shown in Fig. 2, and the solid lines show the experimentally observable Doppler shift shown in Fig. 5.

z = 15 mm. It should be noted that even if a flow in the z-direction exists, the azimuthal Doppler shift can be extracted as the ϕ-dependent component of the Doppler shift. Since the flow velocity is obtained from the amplitude of the sinusoidal variation, the actual flow velocity cannot be determined when the deviation between the broken line and the solid line is significant. Figure 6 clearly shows that as r increases, the rotation effect due to the Gouy phase shift decreases. On the other hand, as r increases, the azimuthal Doppler shift decreases in inverse proportion. Therefore, choosing the experimental parameters that can reasonably reduce the Gouy phase effects is crucial.

4. Feasibility of Transverse Flow Measurement in our Experimental Setup

In this section, we discuss the feasibility of proof-of-principle experiments by performing numerical analysis with the actual parameters of our experimental setup shown in Fig. 7. The LG beam is incident perpendicular to the gas flow. Since the azimuthal Doppler shift is proportional to the topological charge, the higher mode LG beam is preferable for the measurement. However, the diffrac-

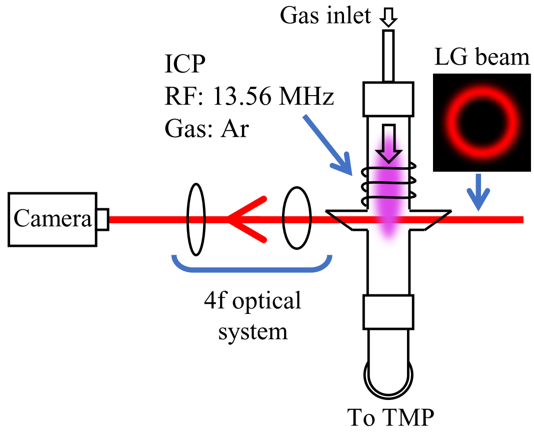

Fig. 7 Schematic diagram of the experimental setup. The LG beam is incident perpendicular to the gas flow, and the 4f optical system transfers the transmitted light to the camera. The spectrum is constructed for each pixel using the camera images recorded during the TDLAS.

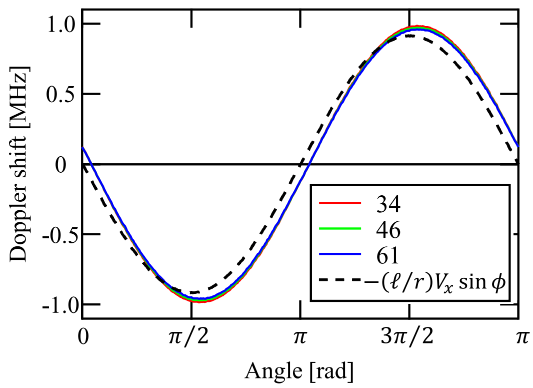

Fig. 8 Absorption coefficient dependence of the observable azimuthal Doppler shift.

tion efficiency of the hologram used for beam mode conversion decreases at large ℓ. Here, we chose $\ell = +10$ as the appropriate value for our setup. After the LG beam propagates while being absorbed in the plasma, the beam image is transferred to the camera by the 4f optical system. Images are recorded while the laser wavelength is swept and used to construct the Doppler spectrum at each pixel. The inner diameter of the discharge tube is 15 mm. Here we evaluate the azimuthal Doppler shift at $r = 262\,\mu$m, which is the radius of the donut-shaped intensity distribution of the LG beam. Figure 8 shows the ϕ-dependence of the azimuthal Doppler shift at $U_x = 150$ m/s and z = 15 mm with the absorption coefficients of 34, 46, and 61 m^{-1} corresponding to the absorption ratios of 40, 50, and 60% for a plane wave with an absorption length of 15 mm, respectively. The other parameters are the same as the calculation for Fig. 4. The amplitude of the Doppler shift variation is about 1 MHz, the deviation due to the absorption coefficient is negligible, and the deviation from $-(\ell/r)U_x \sin\phi$

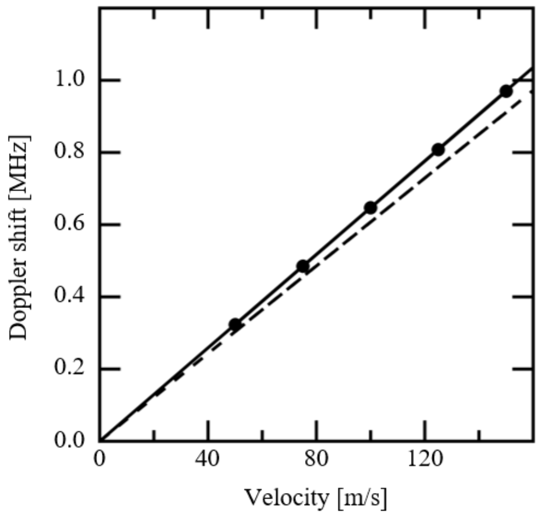

Fig. 9 Relationship between transverse flow velocity and azimuthal Doppler shift.

shown by the broken line is less than 10% for the results obtained with all the absorption coefficients. Therefore, the depth of the anisotropically absorbed intensity structure does not affect the measurement. As shown in Fig. 9, the linearity of the transverse flow velocity and the azimuthal Doppler shift was also confirmed in the range of 50 - 150 m/s. The deviation from $-(\ell/r)U_x \sin\phi$ shown by the broken line is less than 10% over the flow velocity range. These numerical analyses show that our experimental setup can measure the transverse velocity with the Gouy phase effect of less than 10%.

5. Conclusions

We have numerically analyzed the LG beam propagation in the transversely flowing plasma to examine the feasibility of the transverse flow measurement by the LG beam absorption spectroscopy. In the transverse flow, the azimuthal Doppler shift depends on the position in the beam cross-section; therefore, the beam is inevitably absorbed anisotropically. Since the anisotropic LG beam rotates with propagation, the observed Doppler spectra are affected by the rotation. Therefore, it is essential to perform the experiment under the condition that the deviation by the effect can be suppressed to an acceptable level to measure the transverse flow with this spectroscopic method. According to the numerical analysis, the deviation caused by the rotation is reduced to several percent by adequately selecting the position used to evaluate the azimuthal Doppler shift. The numerical analysis was also performed with the parameters of our experimental setup, showing that the transverse flow measurement is possible with more than 90% accuracy in the range of 40 - 60% absorption ratio and 50 - 150 m/s transverse flow velocity. A proof-of-principle experiment is currently underway, the results of which will be reported elsewhere.

Acknowledgments

The authors thank Prof. Y. Toda (Hokkaido Univ.), Dr. Y. Shikano (Gunma Univ.), and Dr. H. Kobayashi (Kochi Univ. Tech.) for the fruitful discussions. This work was supported by JSPS KAKENHI (Grant Numbers 17H03000, 18KK0079, 21H01058) and NIFS Collaborative Research Program (NIFS13KOAP026, NIFS22KIIP010).

[1] B. Clarenbach *et al*., Plasma Sources Sci. Technol. **12**, 345 (2003).
[2] E. Abe *et al*., Plasma Fusion Res. **14**, 1201066 (2019).
[3] M. Aramaki *et al*., AIP Advances **8**, 015308 (2018).
[4] S. Yoshimura *et al*., Plasma Fusion Res. **5**, S2052 (2010).
[5] M.J. Goeckner *et al*., Phys. Fluids B **4**, 1663 (1992).
[6] D. Lee *et al*., Appl. Phys. Lett. **91**, 041505 (2007).
[7] S. Yoshimura *et al*., J. Adv. Sim. Sci. Eng. **9**, 150 (2022).
[8] S. Yoshimura *et al*., Jpn. J. Appl. Phys. **59**, SHHB04 (2020).
[9] A.E. Siegman, *Lasers* (University Science Books, Herndon, 1986), p. 647.
[10] K. Matsushima and T. Shimobaba, Opt. Express **17**, 19662 (2009).
[11] X. Yu *et al*., Opt. Lett. **37**, 4943 (2012).
[12] W. Zhang *et al*., Opt. Lett. **45**, 1543 (2020).
[13] D. Mas *et al*., Opt. Commun. **164**, 233 (1999).
[14] F. Shen and A. Wang, Appl. Opt. **45**, 1102 (2006).
[15] L. Allen *et al*., Opt. Commun. **112**, 141 (1994).
[16] J. Hamazaki *et al*., Opt. Express **14**, 8382 (2006).